International Journal on Advanced Science Engineering Information Technology

Vol.8 (2018) No. 6
ISSN: 2088-5334

Geometric Accuracy Assessment of Very High-Resolution Optical Data Orthorectified using TerraSAR-X DSM to Support Disaster Management in Indonesia

Inggit Lolita Sari#, Sukentyas Estuti Siwi #, Randy Prima Brahmantara#, Haris Suka Dyatmika#, Agus Suprijanto#, Kuncoro Adi Pradono#

Remote Sensing Technology and Data Centre - LAPAN, Jakarta, 13710, Indonesia
E-mail: inggit.lolita@lapan.go.id; iken.lapan@gmail.com; randy.prima@lapan.go.id; haris.suka@lapan.go.id; agus_suprijanto@lapan.go.id; kuncoro.adi@lapan.go.id

***Abstract*— Advanced remote sensing satellite data with detail spatial resolution can be an alternative to aerial photography and outweigh in providing rapid and vast spatial, remote area, and consist of multispectral bands to produce continues information. The various types of very high spatial resolution satellite, benefit in producing information for large-scale mappings, such as updating an urban map and supporting disaster management for mitigation, preparedness, emergency response, and recovery effectively and efficiently. Large-scale mapping information for disaster management, particularly for quick response is essential to map the impacted sites, measure the number of houses and infrastructure damaged and determine the evacuation area. However, in producing large-scale mapping, the information should refer to the geospatial specification standard, such as accurate geometric, detail thematic information and completeness. This study aims to identify the use of Pleiades imagery for supporting large-scale mapping, including for disaster management by assessing the geometry accuracy from a standard product acquired from the ground station and precise orthorectification using different types of DSM, including TerraSAR-X and improvement using ground control points. The results show that the improved accuracy to meet geometric accuracy standard for scale 1:5000 can be achieved using a primary product data which process using an insertion of GCPs and selecting the better DSM, while for the standard ortho product can be achieved using shifting the coordinate position of the image. Assessment of the thematic extraction visually shows that the imagery meets the information for large-scale mapping, but detail attribution requires information from field data.**

***Keywords*— geometric; pleiades; TerraSAR-X; DSM; disaster management.**

I. INTRODUCTION

The devastating earthquake in Lombok Island in August 2018 killed 460 people, evacuated 417,529 people, damaged 71,962 houses, including facilities and caused 7.45 trillion rupiahs loss [1]. Indonesia is a tropical country prone to catastrophe because geographically, it is located at three confluence of tectonic plates, namely Indo-Australia, Pacific plates, and Eurasian, moreover the country located at the ring of fire [2]. The confluence tectonic plates of Indo-Australia and Eurasia span from the west coast of Sumatra to the southern coast of Java and continue to the west part of Sulawesi, while the Pacific plates span from the northern part of Papua to Maluku. This geographic position causes Indonesia is vulnerability to earthquake and tsunami. The other geological hazard also comes from a large number of volcanoes at about 150 spread over Sumatra, Java-Bali-Nusa Tenggara, North Sulawesi, and Maluku, including Papua, causes the country prone to mount eruptions [3]. As a tropical country, Indonesia's climate characteristically has two distinct seasons; monsoon wet and dry with average annual rainfall varies from 1.7 to 3.1 cm, while on the mountainous regions, the rainfall rate reaches up to 6.1 cm [4], [5]. This climate condition causes potential Indonesian risk to natural disasters, such as landslide, floods, and many others.

Report from Indonesia National Agency for Disaster Management (BNPN) shows that in 2017, there were 2,862 disaster events and in the middle of 2018 record, about 1,095 events consist of floods, landslides, volcanic eruptions, earthquakes, and forest fires [6]. The BNPB identify the area of disaster based on the data from official institutions and the analyses of the area impacted is having a minimum of 1 hectare. The loss is from the victims, material loss and environmentally damaged [3]. Therefore, information of the precise location of a disaster site produces in rapid and detail is essential to support disaster management to minimize the loss and for quick recovering.

For several decades, remote sensing has been a reliable data, reaching remote area, provide fast information and for a vast area, and consist of the multispectral band for continuous analysis. Advanced remote sensing data derived from optical very high spatial resolution satellite (VHSRS) and radar can be used for supporting disaster management, such as mitigation, preparedness, emergency response and recovery in effectively and efficiently.

Previous researches on VHSRS for disaster management at the local level can be seen on the application of Quickbird and IKONOS with 0.6 – 1 m which use for mapping rapid urban extent, road and automated building at map scale not smaller than 1:2000. While imagery with 5 m, such as The Indian Remote Sensing (IRS) and SPOT 5 was sufficient to produce information at 1:10000 [7]. Information at local level used for accounting in situ damages, such as houses and building damage is using the method of fuzzy color image segmentation to detect object and analysis the land cover changes using post-processing classification. Assessing geometry quality on the use of VHSRS of Pleiades imagery were also conducted in Cyclades Island, Greece showed that the imagery provides high accuracy for large-scale mapping and benefit for updating base map [8], [9], including to support mapping urban green space for scale 1:5000 [10]. The utilization of radar data using TerraSAR-X and TanDEM-X strip map mode also useful for urban mapping footprint using 12 m resolution data [11].

In 2018, Indonesia's international ground station located in Parepare, South Sulawesi can acquire Pleiades imagery and TerraSAR-X (TSX)/TanDEM-X (TDX) through programming acquisition. The government provides the VHSRS data to support many applications, such as urban map planning and disaster management. Pleiades imagery has 0.5 m spatial resolution and revisits cycle at the same location in the same orbit in 26 days and able to revisit every day in equator region with incidence angle ±30°. Detail specification of Pleiades data is in Table 1.

The TSX/TDX imagery has various modes, one of the image mode is the Stripmap mode which has 3 m spatial resolution can also be able to revisit each day and revisits cycle at the same location in the same orbit in 11 days. This SAR imagery is a benefit for the tropical area due to independent from cloud and time acquisition [12].

The utilization of VHSRS for producing large mapping scale, particularly for geometric assessment has to meet the specification of standard large-scale mapping, which in Indonesia is regulated by the Geospatial Information Agency (BIG). In this research, mainly is to meet the standard for mapping at scale 1:1000 to 1:10000. The large-scale mapping standard also requires the completeness and detail thematic assessment. Therefore, this paper will discuss the use of Pleiades imagery and TSX/TDX imagery in order to support large mapping, moreover for disaster management in Indonesia.

II. Material and Method

Pleiades imagery produced by LAPAN consist of the two-level product; primary product and standard ortho, while the TSX /TDX consist of Single Look Slant Range Complex (SSC) and Enhanced Ellipsoid Corrected (EEC). The Pleiades primary products are a raw product completed with a Rational Polynomial Coefficients (RPCs) and in a bundle of multispectral and panchromatic bands, while the standard ortho products are already in systematically orthorectified and pansharpened.

The SSC of TSX /TDX are in a raw format consist of amplitude and phase information which best for creating interferometry and radargrammetry [13], while the EEC product are already in systematically geometric and terrain corrected. The paired SAR imagery benefit in production DSM.

The accuracy geometry of primary product depends on the availability of GCP and DEM. Processing primary product without GCPs can be build using the Rational Function of RPCs model which can be processed on commercial software such as PCI Geomatics. The RPC created from two rational polynomials which correlate the coordinate of the imagery and the ground. Therefore processing using RPCs user do not have to know the physical parameters of the satellite [15].

This study aims to compare the geometric accuracy produced from the various method of orthorectification processes from data with a different incident angle, DSM and including measuring the improvement using addition manual of Ground Control Points (GCPs) obtained from field survey. Improvement accuracy of standard ortho product will also be measured and achieved using shifting method of the geometric position.

The reference for assessing the geometric accuracy for large-scale mapping is based on the Geospatial Information Agency (BIG) law, with accuracy minimum 5 m for map 1:10000 and 2.5 m for 1:5000 for level 3 [16]. Measurement on the geometric accuracy as provided in the equation of CE measurement, while the geometric accuracy standard for the base map (in meters) are in Table 2.

TABLE 1
SPECIFICATION OF PLEIADES 1A/1B

Mode Imaging	Panchromatic	Multispectral
Spatial resolution	0.5 m GSD at the nadir	2 m GSD at the nadir
Spectral range	480 – 830 nm	Blue (430 –550 nm) ; Green (490 –610 nm) ; Red (600 – 720 nm) ; Near Infrared (750 –950 nm)
Swath Width	20 km at nadir	
Off-Nadir imaging	Up to 47°	
Radiometric range	12 bit per pixel	
Revisit frequency	2 days for combine Pleiades 1A & 1B	
Altitude	694 km	

Mode Imaging	Panchromatic	Multispectral
Orbit	Sun-synchronous, 10:15 A.M	
Geometric accuracy	- Primary product GCP and perfect DEM has 0.30 m CE90 - Standard ortho product: 8.5 m CE90 at nadir has ± 10.5m at 30°	

Source: [12],[14]

TABLE II
THE GEOMETRIC ACCURACY STANDARD FOR THE BASE MAP [16]

No	Scale	CI	Geometric Accuracy					
			Level 1		Level 2		Level 3	
			H (CE90)	V (LE90)	H (CE90)	V (LE90)	H (CE90)	V (LE90)
1.	1:1000000	400	200	200	300	300	500	500
2.	1:500000	200	100	100	150	150	250	250
3.	1:250000	100	50	50	75	75	125	125
4.	1:100000	40	20	20	30	30	50	50
5.	1:50000	20	10	10	15	15	25	25
6.	1:25000	10	5	5	7.5	7.5	12.5	12.5
7.	1:10000	4	2	2	3	2	5	5
8.	1:5000	2	1	1	1,5	1.5	2.5	2.5
9.	1:2500	1	0.5	0.5	0.75	0.75	1.25	1.25
10.	1:1000	0.4	0.2	0.2	0.3	0.3	0.5	0.5

*CI = Contour Interval, H= Horizontal, V= Vertical, CE 90=Circular Error 90% accurate

Measurement of CE is as follows;

$$CE90 = 1{,}5175 \times RMSE_r \quad (1)$$

$$LE90 = 1{,}6499 \times RMSE_z \quad (2)$$

Where :

$RMSE_r$ = *Root Mean Square* at x and y (horizontal)

$RMSE_z$ = *Root Mean Square* at z (vertical)

The study area is located in Madiun and Magetan regency at 7°28′38.65″S - 7°51′9.82″S and 111°11′54.68″E - 111°41′43.69″E with the topographic elevation ranging from 0 to 2,000 m. The area is prone to natural disaster, such as landslide and flooding. A total of 32 natural disaster events in Madiun in 2016 (Madiun Regional Disaster Management Agency/BPBD) and more critical to Magetan with 43 events for 3 months during January – March 2017 (Magetan Regional Disaster Management Agency/BPBD). However, both regencies are mostly located in a plain area at 0-2%, while some area has steep at more than 40%.

Three Pleiades imagery scenes were acquired in 2017 with an incidence angle ranging from 13°–22°. The data were produced in primary and standard ortho. The DSM for the comparison were TSX, ALOS PALSAR, and SRTM. The TSX DSM is in 9 m spatial resolution and SRTM 30 m from BIG, and ALOS PALSAR DSM with 12,5m can be downloaded from JAXA. (Dataset: ASF DAAC 2015, ALOS PALSAR_Radiometric_Terrain_Corrected_high_res; Includes Material © JAXA/METI, 2007. Accessed through ASF DAAC, 11 July 2018).

The geometric reference obtained from the field survey. From 34 points collected from dGPS Garmin Geo7X where the accuracy in the field is between 0.01 cm and 15 cm. These points later divided into 24 points for GPCs and 10 points of Independent Control Points with the distance each point around 2-5 km. The study area and distribution of GCPs/ICPs can be seen in Fig. 1.

The steps of systematically orthorectification processed using rational function model and the improvement of the primary level products were processed using refining the RPCs by addition of GCPs and processed using Toutin Rigorous Model [17]. This method is superior for improving geometric accuracy which can be processed using PCI Geomatics.

Assessment of horizontal geometry measure as follows;

$$RMSE_{horizontal} = \sqrt{\frac{D^2}{n}} \quad (3)$$

$$D^2 = \sqrt{RMSEx^2 + RMSEy^2}$$

$$= \sqrt{\Sigma[(x_{data} - x_{chek})^2 + (y_{data} - y_{chek})^2]}$$

Where: n is total field surveyed points; D is the difference between field surveyed coordinates and map coordinates; x is coordinate in X (Easting); y is coordinate in Y (Northing).

The next step is to identify the information extracted from Pleiades imagery to fulfill the land cover classes/object for map 1:5000 to 1:10000 which is determined by the Indonesia National Standard (SNI) with number 19-6502.1-2000. Assessment of the thematic information processed by comparing the reference map of detail urban planning from local government and Pleiades imagery.

Identification of minimum building/houses identified is based on SNI 03-1733-2004 which stated that the minimum house which is measured by the concrete floor for one family (5 persons) in Indonesia is at 51 m^2.

III. RESULT AND DISCUSSION

Assessment of the geometry accuracy of orthorectification imagery is based on field coordinate. Based on the process to build the orthorectification using different incidence angle data, and different DSM, the result of the statistics displacement from those 4 types of orthorectification process can be seen in Table 3 and Fig. 2.

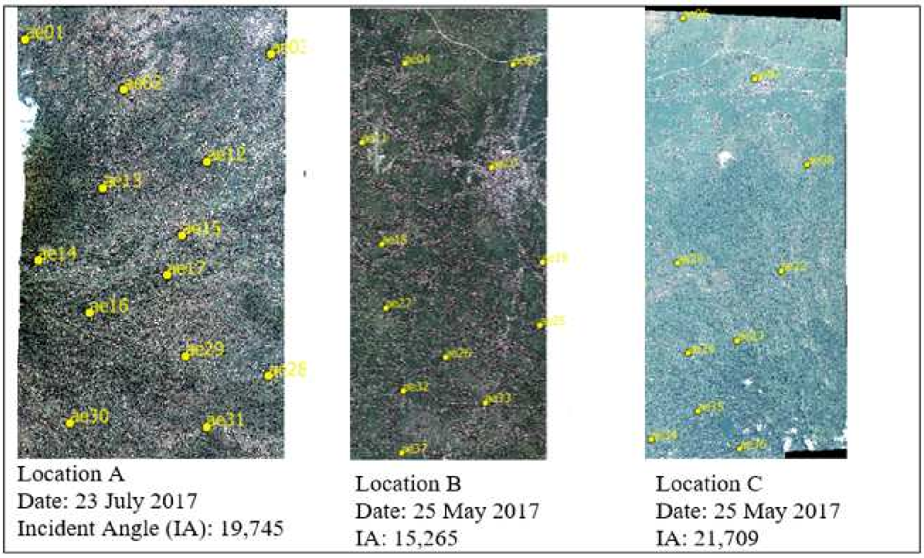

Fig. 1 Distribution of GCPs and ICPs on three scenes of Pleiades imagery and its different incident angle

TABLE III
STATISTICS DISPLACEMENT FROM 4 TYPES OF SYSTEMATIC ORTHORECTIFICATION PROCESS

Location Scene	**Incident angle**		**Standard Ortho Product**		**Primary using DSM TSX (Without GCP)**		**Primary using DSM ALOS PALSAR (Without GCP)**		**Primary using DEM SRTM (Without GCP)**	
			X	**Y**	**X**	**Y**	**X**	**Y**	**X**	**Y**
A	19,745	Min	-2.286	-2.875	-0.113	-4.004	0.393	-4.439	-7.071	-3.27
		Max	6.516	0.844	3.391	0.200	3.292	0.084	-5.430	0.263
		Std	2.118	0.860	1.120	1.184	0.944	1.243	0.528	0.995
		RMSE	3.067		2.688		2.764		6.228	
		CE90	4.655		4.079		4.195		9.452	
B	15,265	Min	1.892	-0.156	1.168	-2.151	0.005	-1.584	-0.833	-8.120
		Max	6.477	3.821	6.173	1.572	5.219	2.404	3.962	9.034
		Std	1.300	1.026	1.236	1.088	1.343	1.031	1.252	4.225
		RMSE	3.877		3.675		3.308		6.144	
		CE90	5.883		5.577		5.020		9.323	
C	21,709	Min	1.609	0.823	1.770	-3.551	2.053	-3.798	-3.606	-10.744
		Max	6.407	6.816	5.492	3.495	5.157	2.664	0.812	-4.852
		Std	1.439	1.821	1.262	2.013	0.932	1.768	1.484	1.813
		RMSE	5.562		3.940		3.693		9.714	
		CE90	8.440		5.979		5.605		14.741	

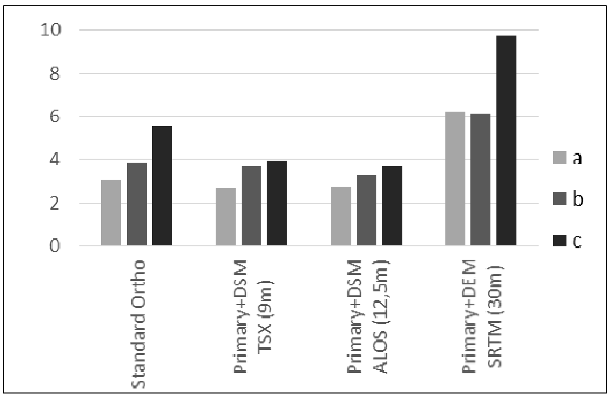

Fig. 2 The comparison displacement in CE90 from 4 types of orthorectification process

TABLE IV
COORDINATE AND DISPLACEMENT IN LOCATION C

No.	Elevation (meters)	Field coordinate		Standard ortho product		Displacement (meters)
		Easting	Northing	Easting	Northing	
ae06	90.406	566106.043	9171320.642	566104.434	9171318.881	2.385
ae07	99.650	571950.844	9166384.712	571946.639	9166383.506	4.375
ae08	149.676	576214.896	9159398.774	576209.640	9159397.951	5.320
ae20	209.808	565698.103	9151367.935	565691.931	9151361.119	9.196
ae22	418.535	574080.155	9150763.736	574076.263	9150762.096	4.224
ae23	641.889	570547.296	9145061.528	570542.064	9145057.946	6.340
ae24	413.777	566590.797	9144039.132	566586.725	9144035.966	5.158
ae34	335.143	563535.892	9136978.512	563529.485	9136975.927	6.909
ae35	634.787	567330.183	9139294.202	567325.232	9139290.549	6.153
					RMSE	5.562
					CE90	8.440

Table 3, 4 and Fig. 2, shows that the highest displacement occurred in the location C, which is located in the mountain area, and the incidence angle is larger than the other scenes. This because the RPCs is dependent on relief [18] which also can be seen that in Location B is relatively in flat topography. Therefore the RPCs method will produce better accuracy.

In general, the highest accuracy for precise orthorectification using RPCs without GCPs using different DSM/DEM showed that the highest accuracy resulted from TSX, followed by ALOS PALSAR DSM. The ALOS PALSAR is categorized as s medium-resolution spatial sensors [19]. This can be concluded that data with incident angle is less than 20 degrees processed with systematically orthorectification is entirely suitable for scale 1:10000 to 1:25000, including for imagery from standard ortho product. While analysis for highest displacement due to topographic and incident angle occurred in location C which analysis for each point can be seen in Table 4 and Fig. 3.

Improvement on geometric accuracy for standard ortho and primary product in order to meet the substantial scale map standard, in this research shows that can be achieved by processing using an insertion of GCPs/refinement for primary product, while an improvement for standard ortho can be achieved by shifting the geometric position of the imagery.

Fig. 4 showed that based on statistics and a visual assessment on the quality of DSM TSX and ALOS PALSAR, the TSX DSM has more detail resolution, which then will determine the accuracy of the orthorectification results compare to the lower DEM resolution (such as SRTM) as the input of elevation data. The comparison DSM from TSX 9 m resolution and ALOS PALSAR DSM 12.5 m can be seen in Fig. 4.

While Refinement RPCs by using the addition of GCPs can fulfill the standard geometric accuracy for 1:5000 which shows in location B, which can be seen in Fig. 5 and Table 5.

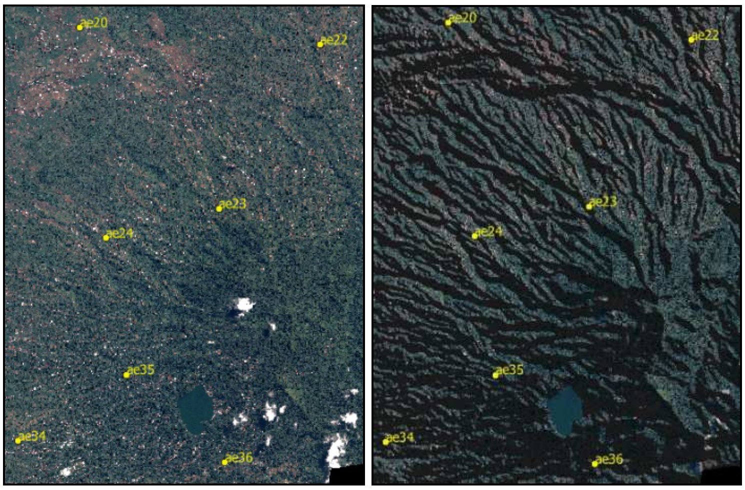

Fig. 3 The highest CE in Location C occurred for points located at number 20, 22, 23, 24, 34, 35

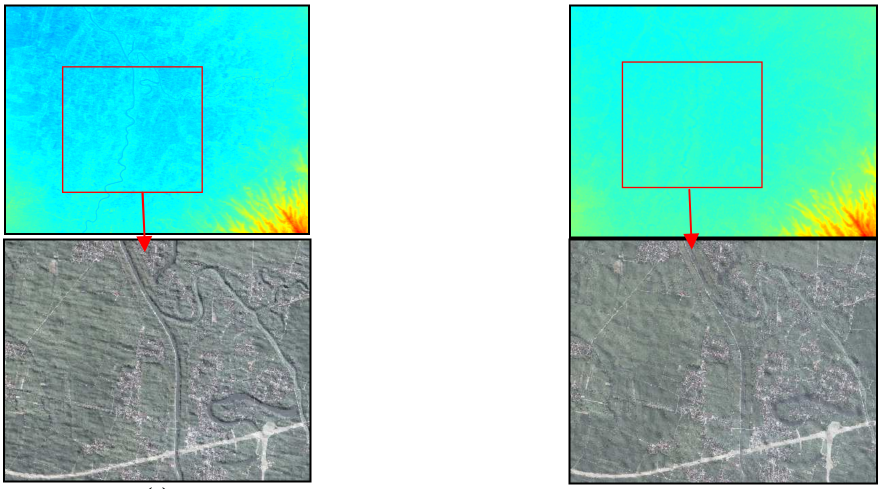

(a) (b)

Fig. 4 Comparison of a) TSX DSM (9m) and b) ALOS PALSAR DSM (12.5 m)

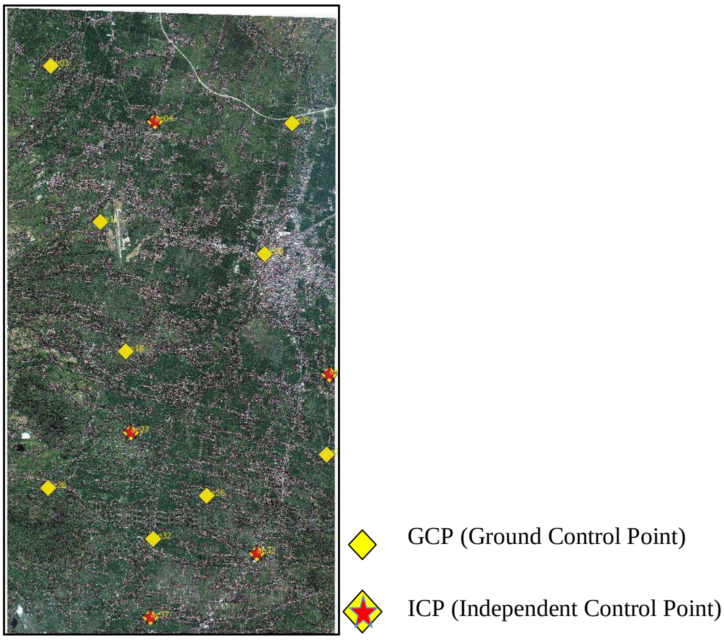

Fig. 5 Distribution of GCPs and ICPs in Location B

TABLE V
PRIMARY USING TSX WITH GCP IN LOCATION B

No.	Elevation (meters)	Field coordinate		Standard ortho product		Displacement (meters)
		Easting	Northing	Easting	Northing	
ae04	91.36	550054.5653	9165080.5	550055.000	9165080.5	0.434
ae19	122.01	561066.9303	9149153.4	561067.503	9149153.5	0.578
ae27	118.10	548548.3225	9145486.2	548548.499	9145486.5	0.341
ae33	160.84	556511.7361	9137880.1	556510.493	9137879.0	1.668
ae37	120.29	549802.7066	9133834.9	549803.488	9133835.0	0.784
					RMSE	0.898
					CE 90	1.363

On the other hand, geometric accuracy for standard ortho product can be improved using the shifting method. This because the displacement shows a pattern of systematic direction which can be seen in Table 6.

TABLE VI

MEASUREMENT AND DIRECTION OF DISPLACEMENT OF STANDARD ORTHO PRODUCT COMPARE WITH A COORDINATE ON FIELD SURVEYED (METERS)

Location A			**Location B**			**Location C**		
No.	**X**	**Y**	**No.**	**X**	**Y**	**No.**	**X**	**Y**
ae01	-2.286	-0.281	ae04	3.015	1.624	ae06	1.609	1.761
ae02	3.274	0.844	ae05	6.477	1.047	ae07	4.205	1.206
ae03	3.465	-0.382	ae10	4.416	1.636	ae08	5.256	0.823
ae12	2.504	-0.793	ae11	3.053	1.539	ae20	6.172	6.816
ae13	6.516	-0.096	ae18	2.225	1.631	ae22	3.892	1.640
ae14	1.770	0.178	ae19	4.550	3.821	ae23	5.232	3.582
ae15	2.096	-0.972	ae25	1.892	2.565	ae24	4.072	3.166
ae16	3.168	-2.875	ae26	2.045	0.928	ae34	6.407	2.585
ae17	2.205	-0.420	ae27	2.653	0.291	ae35	4.951	3.653
ae28	0.915	-0.607	ae32	3.605	0.954			
ae29	3.413	-0.797	ae33	4.060	1.411			
ae30	4.970	-1.134	ae37	3.579	-0.156			
ae31	0.884	-0.881						

TABLE VII

IMPROVEMENT ACCURACY FOR STANDARD ORTHO PRODUCT USING SHIFTING METHOD FOR LOCATION B.

Displacement in X (meters)	**Displacement in Y (meters)**	**RMSE h**
0.994	1.079	1.079
1.729	1.747	1.747
1.272	1.279	1.279
2.160	2.383	2.383
0.238	0.563	0.563
3.702	4.193	4.193
0.102	0.287	0.287
1.502	1.506	1.506
1.021	1.077	1.077
2.027	2.410	2.410
4.506	4.514	4.514
1.386	1.663	1.663
	RMSE	1.892
	CE90	2.871

The shifting method has a benefit for improving the accuracy because requiring less/few GCPs. This research shows that the shifting of the standard ortho product could increase the geometric accuracy (in CE) from 5.883 to 2.871 m. The result can be seen in Table 7 above.

This we can conclude that based on Table 5 shows the improvement of geometric accuracy in order to meet the standard mapping scale for 1:5000 can be achieved for a primary product which processed by using an insertion of GCPs and selecting the better DSM. While improvement of the standard ortho product can be achieved using shifting the position calculated from the reference image/base GCPs as can be seen in Table 7. The shifting process for geometric improvement can be run automatically.

Analysis of the quality information of feature extracted from Pleiades imagery was analyzed using the visual method with the reference map of the local government map in large-scale mapping 1:5000. This is Fig. 6 shows that the houses can be accounted and delineated using Pleiades imagery, where the small settlement size is at 6-60 m^2.

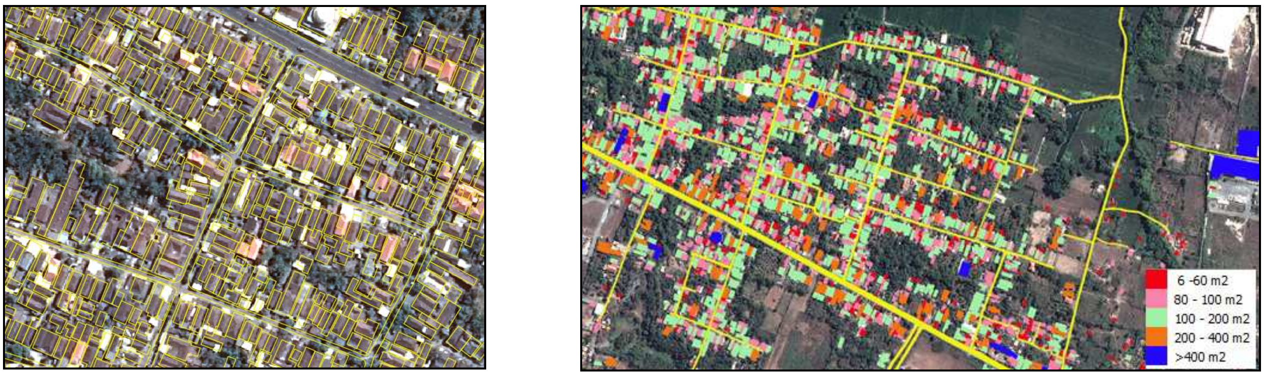

(a) (b)

Fig. 6 Assessing feature extracted from Pleiades imagery for large scale map using the reference map shows building and road delineation

While based on the quality of precision and accuracy of delineation resulted from the orthorectification processed to support extracting feature for large-scale mapping 1:5,000, can be seen in Fig. 7. The figure shows that Pleiades imagery is able to delineate for an object with an area less than 45 m^2. However, accuracy on thematic and attribution should be completed through validation in the field due to the limitation of information/attribution extracted from the optical imagery. This because building and settlements were identified by the roof not identified for the function of the building. Moreover, typical of settlements are in densely populated and close together causes challenging to process in digital classification for its individual building as shown in Fig. 8. While several features that can be detected from Pleiades imagery for scale 1:5000 is determine based on SNI 19-6502.1-2000 and for detail, planning map is based on Indonesian Government Law No. 8, 2013, as can be seen in Fig. 9.

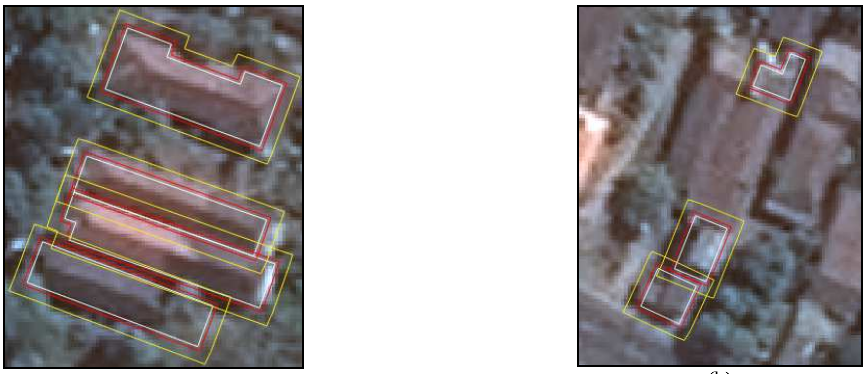

(a) (b)

Fig. 7 Delineation accuracy for building from the reference map in white and red as tolerance accuracy for 0.5m from reference (for level 2 map scale standard), yellow as tolerance accuracy for 2m from the reference map (for level 3 map scale standard), while image b) shows the building delineation for area less than 45 m^2

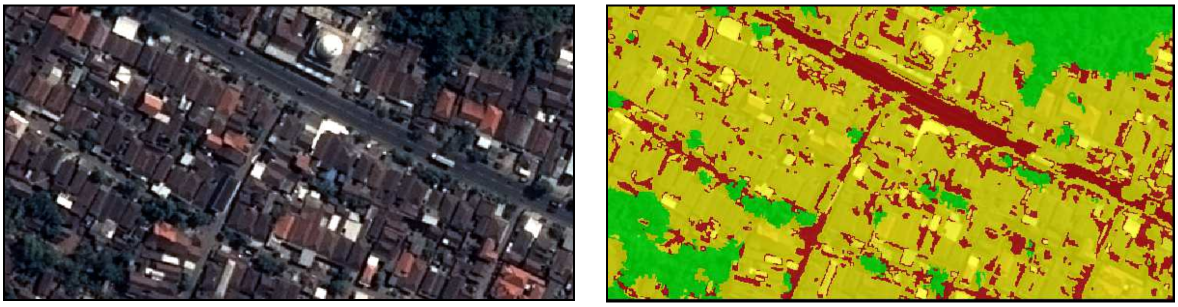

Fig. 8 Settlements mapping using the segmentation method

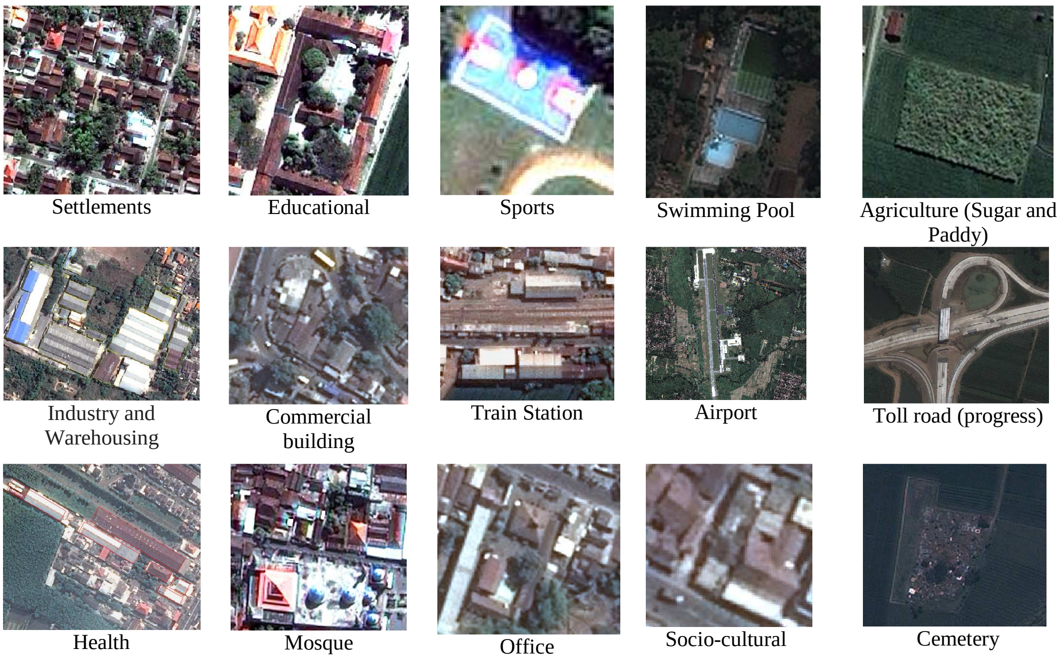

Fig. 9 Several features extracted at scale 1:5000

(a) Before (b) After

Fig. 10 Building loss detected after Lombok earthquake from Pleiades imagery acquired on a) 1 May 2018 and b) 7 August 2018

This research shows that Pleiades imagery has fulfilled the standard in supporting large-scale base map and updating the large-scale map. In supporting the disaster management, information on spatial area impacted and counting the number of building loss can be seen in the case of Lombok Island disaster event. This natural disaster is caused by the series of the earthquake. An analysis of the building loss is measured using the imagery from before and after of the disaster event provided by the imagery acquired from LAPAN, as can be seen in Fig. 10. The imagery is successfully acquired and processed within 2 days after the disaster occurred.

Analysis on the use of Pleiades imagery and TSX/TDX with its agility which can be programming, and has a high geometric accuracy, ability to provide detail thematic information which will be one of the original national data is critical data to support a national program, particularly in disaster management. This VHSRS benefit to give precise and up to date information on the disaster impact extent, so the rescuing team will able to start identifying the infrastructure to rescue and evacuate people. However, an improvement in automatic classification to detect the object by combining various data, method, and modeling should be a focus to support active disaster management.

IV. Conclusions

Pleiades imagery with 0.5 m spatial resolution suitable to support large-scale mapping, this can be seen by an assessment on the geometric accuracy and thematic extraction. Pre-processing on improving the geometric accuracy can be divided based on the types of two-level product produced by the ground station. Improvement accuracy to meet standard mapping scale for 1:5000 can be achieved using a primary product data which processed by using an insertion of GCPs and selecting the better DSM, while the improvement of the standard ortho product can be achieved using shifting the coordinate position. Assessment of the thematic extraction detected visually shows that the imagery meet the information for large-scale mapping standard, requires field data for attribution. The DSM could be processed using the paired of the TSX/TDX. Nevertheless, for the detail, automatic classification and building modeling in order to support disaster management require further research.

Acknowledgments

This research was financed by the Ministry of Research, Technology and Higher Education (RISTEKDIKTI) in the INSINAS 2018 scheme. All the author would like to thank the Technology and Data Center – LAPAN for data and facilities, BIG for data support, the local government and especially to the management of INSINAS Flagship LAPAN.

References

[1] BNPB. Dampak Gempa Lombok: 460 Orang Meninggal Dunia dan Kerugian Ekonomi 7,45 Trilyun Rupiah (Lombok Earthquake causes 460 people killed, and 7.45 Trillion Rupiah Economic Loss) 2018.

[2] Mukhlis T, Teukusyakur Dbd, Anhorn J. School Preparedness and Training for Geological Hazard Mitigation: An Example from Indonesia. Disaster Management and Human Health Risk V: Reducing Risk, Improving Outcomes. 2017;173:113.

[3] Robi Amri, Gita Yulianti, Ridwan Yunus, et.al. Indonesia Risk Disaster In Indonesia National Agency for Disaster Management, the editor. 2016.

[4] Dmitriev E. Classification of the forest cover of Tver oblast using hyperspectral airborne imagery. Izvestiya, Atmospheric and Oceanic Physics. 2014;50(9):929-42.

[5] Hidayat R, Ando K, Masumoto Y, Luo J, editors. Interannual variability of rainfall over Indonesia: Impacts of ENSO and IOD and their predictability. IOP Conference Series: Earth and Environmental Science; 2016: IOP Publishing.

[6] Indonesia National Agency for Disaster Management (BNPB). Information Data Natural Disaster in Indonesia: BNPB; 2018.

[7] Li J, Li Y, Chapman MA. High-resolution satellite image sources for disaster management in urban areas. Geo-information for Disaster Management. 2005:1055-70.

[8] Agrafiotis P, Georgopoulos A. Comparative Assessment of Very High-Resolution Satellite and Aerial Orthoimagery. The International Archives of Photogrammetry, Remote Sensing and Spatial Information Sciences. 2015;40(3):1.

[9] Alrajhi M, Janjua KS, Khan MA, Alobeid A. Updating Maps Using High-Resolution Satellite Imagery. The International Archives of Photogrammetry, Remote Sensing and Spatial Information Sciences. 2016;41:711.

[10] Sukojo BM, Nabilah S, editors. Analysis of Accuracy Orthorectification Pleiades and QuickBird Imagery to Creation of Based Map of Detail Spatial Plan for Open Green Space (Case Study: Part of Tuban Urban Area). IOP Conference Series: Earth and Environmental Science; 2018: IOP Publishing.
[11] Felbier A, Esch T, Heldens W, Marconcini M, Zeidler J, Roth A, et al., editors. The global urban footprint—Processing status and cross-comparison to existing human settlement products. Geoscience and Remote Sensing Symposium (IGARSS), 2014 IEEE International; 2014: IEEE.
[12] AIRBUS DS. Pleiades User Guide and Application Guide 2018.
[13] De Oliveira CG, Paradella WR, Da Silva AdQ. Assessment of radargrammetric DSMs from TerraSAR-X Stripmap images in a mountainous relief area of the Amazon region. ISPRS Journal of photogrammetry and remote sensing. 2011;66(1):67-72.
[14] Gim JH, Shin SH. Evaluating positional accuracy of Pleiades 1A satellite imagery in exploiting foreign natural resources. Spatial Information Research. 2016;24(2):85-92.
[15] Fraser C, Hanley H, Yamakawa T, editors. Sub-meter geopositioning with Ikonos GEO imagery. Proceedings of Joint ISPRS Workshop on High-Resolution Mapping from Space; 2001: Hannover, Germany.
[16] Head of BIG. The accuracy of Base Map. In: Geospatial Information Agency (BIG), editor. No 15 the Year 2014. Cibinong: The Ministry of Law and Human Rights of Indonesia.
[17] Deng H, Huang S, Wang Q, Pan Z, Xin Y. Geometric accuracy assessment and correction of imagery from Chinese earth observation satellites (HJ-1 A/B, CBERS-02C, and ZY-3). The International Archives of Photogrammetry, Remote Sensing and Spatial Information Sciences. 2014;40(2):71.
[18] Aguilar M, Agüera F, Aguilar F, Carvajal F. Geometric accuracy assessment of the orthorectification process from very high-resolution satellite imagery for Common Agricultural Policy purposes. International journal of remote sensing. 2008;29(24):7181-97.
[19] Alganci U, Besol B, Sertel E. Accuracy Assessment of Different Digital Surface Models. ISPRS International Journal of Geo-Information. 2018;7(3):114.